## Supplementary Materials and Methods

### Immunohistochemistry

Tumor tissue microarrays containing paired primary lung tumors and corresponding lymph nodes from 40 patients were purchased from US Biomax (LC814a, US Biomax). Immunohistochemistry (IHC) was carried out with recombinant rabbit monoclonal anti-AXL antibody (Abcam) on VENTANA BenchMark ULTRA automated platform (Roche Diagnostics) (1). A semiquantitative analysis of the cytoplasmic expression of AXL protein was performed in 300–500 cells using the Allred scoring system based on staining intensity (0–3) and extent (0–5). Scores of 0–2 were regarded as negative, and scores of 3–8 were considered positive (2).

### *In silico* analyses

Clinical information and RNA-seq data of The Cancer Genome Atlas (TCGA) samples were downloaded from the Center for Molecular Oncology at Memorial Sloan-Kettering Browser (http://www.cbioportal.org). High gene expression was defined as a *Z* score >1 (*AXL*) of the lung cancer cohort (3,4). Kaplan–Meier curves were created in the R software package to determine overall and disease-free survival outcomes for patients with lung adenocarcinoma.

### *In vitro* phenotypic assay

A549 and H2009 cells were treated with a range of TP-0903 does over the course of 72 hr. Proliferation and migration curves were generated using IncuCyte ZOOM (Essen BioScience) with images acquired every 3 hr over a 72 hr timeframe. Images were captured per well for each time point. Data were normalized to controls, and values for 50% inhibitory concentration were calculated using Prism V8.0 (GraphPad software).

**Xenograft study of TP-0903 treatment**

Animal study procedures and experimental design were reviewed and approved for ethical consideration by an internal review committee at Tolero Pharmaceuticals, Inc. Mouse xenografts were implanted subcutaneously in the hind flank of the athymic nude mice. Tumor volumes were grown to a medium size (~100 $mm^3$) before stratification and dose initiation. General health, tumor volumes, and bodyweights were followed over the course of the study. Treatment of oral TP-0903 doses was administered to mice at two dosing levels: 80 mg/kg daily and 120 mg/kg twice weekly dosing over 21 days.

**Capillary Western immunoassay (WES)**

Protein lysates of A549 and H2009 cells were prepared in radio-immunoprecipitation assay buffer (Thermo Fisher Scientific). Proteins were then analyzed in 12-230 and 66-440 kDa WES separation module of quantitative capillary Western immunoassay system (Protein Simple). The following antibodies were used: 1) AXL, AKT, JNK, p38 MAPK, MEK1/2, P42/44 MAPK, and GAPDH (Cell Signaling Technology); and 2) p-AXL and YAP1 (R&D Systems). Protein expression levels were normalized with GAPDH as loading controls.

**RNA-seq**

RNA was extracted from TP-0903 treated and untreated cells or from sh*AXL* knockdown and vehicle control cells in two biological replicates by using the PureLink RNA Mini Kit (Thermo Fisher Scientific). Sequencing of cDNAs was performed with Illumina HiSeq3000 as per manufacturer's instructions. Paired-end FASTQ files were generated and aligned with the human reference genome GRCh38 by using STAR alignment software (5). The RSEM software was applied to quantify expression levels, and fragments per kilo base of transcript per million (FPKM) mapped reads were calculated. Differential expression levels of genes were compared between control and treatment groups by RSEM(6). After filtering genes with low FPKM values (<10), candidate

genes were divided into upregulated (≥1.5-fold) and downregulated (≥1.2-fold) groups. Both sets were used to perform pathway enrichment analysis on Gene Ontology Consortium (http://geneontology.org/) by using Reactome pathway databases in PANTHER (7,8). Heat maps were generated by using Z score, normalized fragments per kilo base million (FPKM) value. The EMT gene set was derived from dbEMT2 (http://dbemt.bioinfo-minzhao.org/) and the cancer stemness gene set from CSCdb (http://bioinformatics.ustc.edu.cn/cscdb/) (9,10).

**Data availability**

RNA-seq for this study is available through the Gene Expression Omnibus (GEO) under accession number GSE128417.

**Analysis of peripheral blood mononuclear cells (PBMCs)**

Peripheral blood were collected before surgery and within 2 hours of lung tumor resection. PBMCs of patient #006 was isolated using prewarm Ficoll-Paque™ PLUS (GE healthcare Life Science) according to the manufacturer's protocol. After centrifugation, PBMCs were transferred into 8 ml advance DMEM, and cells were spun down (200g for 5 minutes). Supernatant removed and PBMCs collected for CyTOF analysis. Circulating tumor cells were identified by gating $CD45^{-}$ /$CK8/18^{+}$/$EpCAM^{+}$ subpopulation from PBMCs (Supplementary Fig. S16A).

**Western blot analysis**

A549 and H2009 were cultured and treated with TP-0903 and/or ruxolitinib over 72 hr. Cell lysates were harvested using RIPA buffer. The concentration of protein lysates was determined by Pierce™ BCA Protein Assay Kit (Thermo fisher). Forty micrograms of the total protein extracts were separated by NuPAGE™ 4-12% Bis-Tris Protein Gels (Thermo fisher) and transferred to PVDF membrane. The membrane was then blocked with 5 % of Blotting-Grade Blocker (BioRad) in TBST and probed using primary antibodies including: 1) oncogenic pathways: JAK1, pSTAT3,

STAT3, pAKT and pERK1/2 (Cell Signaling Technology; 3344S, 9131S, 9139T, 4060, 4377S); 2) cancer stemness markers: CD133 and ALDH1A1 (Cell Signaling Technology; 64326S and 54135S); and 3) EMT markers: Vimentin (Novus; NBP1-92687), N-cadherin, EpCAM (Abcam; ab71916) and CK8/18 (Novus; NBP2-44930); 4) loading control: GAPDH (Cell Signaling Technology; 2118S). Membrane was incubated in HRP-linked secondary antibodies following dilution with TBST (1:5000) at room temperature for one hour. Blots were developed using Western Lightning Plus-ECL Chemiluminescent Reagents (Perkin Elmer, Waltham, MA) and Syngene G:BOX Imaging System.

**Statistical analysis**

Software for RNA-seq analysis included R (version 3.6.0), downloaded from the official R website (https://www.r-project.org/) and program implemented in R studio (Version 1.2.1335) downloaded from R studio website (https://www.rstudio.com/). Multi-group statistical significance was tested by using Duncan multiple range test comparing pre- and post-treated cell lines, with statistical significance as identified.

## Supplementary Figures

**Supplementary Figure S1.**

AXL expression in lung cancer cell lines, primary tumors, and xenografts. **A,** AXL expression pattern was examined in primary tumors and lymph nodes (*left panel*) and quantified using IHC scores (*right panel*). **B**, *AXL* expression levels of 506 samples from The Cancer Genome Atlas (TCGA) cohort according to clinical stages (I, II, III, and IV) (*left panel*). Normalized *AXL* expression levels in the TCGA cohort were grouped by four clinical stages (*right panel*). **C,** Kaplan-Meier curves of overall survival probability and disease-free survival probability were compared between high (*Z* score > 1) and low (*Z* score < 1) expression levels of *AXL*. **D,** Fifty-percent maximal inhibitory concentration ($IC_{50}$) of TP-0903 was generated from proliferation curves of A549 and H2009 cells. $IC_{50}$ values of A549 and H2009 cells were calculated as 31.65 nmol/L and 35.53 nmol/L respectively. **E,** Anti-proliferative effect of TP-0903 on A549 cells at concentrations ranging from 0.1 to 100 nmol/L (three biological repeats). Quantitative analysis of cell growth over 72 hr period following drug treatment (Duncan multiple range test; *, $p < 0.05$; ***, $p < 0.001$). **F,** Proliferation curve of *AXL* knockdown in A549 cells over 48 hr (Duncan multiple range test; ***, $p < 0.001$). **G,** Tumor volume curves based on two dosing regimens of TP-0903 (120 mg/kg bi-weekly and 80 mg/kg daily dosing for 21 days) and vehicle control (*left panel*) in A549 mouse xenograft models. Body weight curve for xenograft models over 30-day treatment course of TP-0903 and vehicle control (*right panel*).

**Supplementary Figure S2.**

Alterations of TGF-β, JAK1-STAT3, cancer stemness, and EMT programs in lung cancer cells treated with TP-0903. **A,** Capillary Western immunoassay (WES) of total AXL and phosphorylated AXL in A549 and H2009 cells treated with or without 40 nmol/L TP-0903 or in sh*AXL* knockdown A549 cells and vehicle control. **B,** Schematic illustration of transcriptomic analysis procedures. **C,**

Expression heat maps and Venn diagrams of down- and up- regulated genes in cells treated with TP-0903 and in *AXL* knockdown cells. **D,** Reactome pathway enrichment analysis (PANTHER) of downregulated genes intersected in TP-0903-treated and *AXL* knockdown cells, categorized in oncogenic pathway, cell cycle and DNA repair, and cellular function. False discovery rate (FDR): $p < 0.05$. **E,** PANTHER of upregulated genes intersected in TP-0903-treated and *AXL* knockdown cells, categorized in oncogenic pathway, extracellular matrix, cell-cell interaction, and cellular function. FDR: $p < 0.05$. **F & G,** Expression heat maps of genes related to epithelial-mesenchymal transition (EMT) and cancer stemness.

**Supplementary Figure S3.**

Capillary Western immunoassay (WES) of proteins associated with TGF-β, PI3K/AKT/mTOR, JNK/p38 MAPK and Ras/RAF/MEK pathways.

**Supplementary Figure S4.**

Raw data of capillary Western immunoassay represented in supplementary Fig.S2A and Fig.S3

**Supplementary Figure S5-14.**

Cytometry by Time-of-Flight (CyTOF) analysis of oncogenic signaling components, cancer stemness, and epithelial-mesenchymal transition (EMT) markers in Patient 004, 006, 007, 008, 009, 010, 012, 014, 016, and 017 (see Fig. 1H-L for Patient 002). **A,** t-distributed stochastic neighbor embedding (*t*-SNE) scatter plot of subpopulations. *t*-SNE scatter plots of expression intensity of markers for oncogenic signaling (**B**), cancer stemness (**C**), and EMT (**D**) among different cell populations sets.

**Supplementary Figure S15.**

Western blots of proteins associated with oncogenic pathways, cancer stemness, and epithelial-to-mesenchymal transition (EMT) in TP-0903 and/or ruxolitinib. Two isoforms of EpCAM in A549 were detected similar to those of a previous study (11).

**Supplementary Figure S16.**

Cytometry by Time-of-Flight (CyTOF) analysis of oncogenic signaling components, cancer stemness, and epithelial-mesenchymal transition (EMT) markers in tumor cells and circulating tumor cells (CTCs) of Pt 006. **A,** CTCs were identified as $CD45^{-}/CK8^{+}/18^{+}/EpCAM^{+}$ subpopulations from peripheral blood mononuclear cells. **B,** t-distributed stochastic neighbor embedding (*t*-SNE) scatter plot displaying 15 subpopulations derived from primary tumors and CTCs (arrow) from Pt 006. *t*-SNE scatter plots of expression intensity of markers for oncogenic signaling (**C**), cancer stemness (**D**), and EMT (**E**) among these subpopulations.

## Supplementary Table S1. Clinicopathological information of lung cancer patients

| Patient ID | Age | Gender | Smoking status | Lung cancer type and specimen | Subtype | Differentiation | TNM classification | Stage | Max tumor size | EGFR | ALK | ROS1 | Organoid culture |
|---|---|---|---|---|---|---|---|---|---|---|---|---|---|
| Pt 002 | 80 | F | Former smoker, quit 25 years ago | Adenocarcinoma (lymph node metastasis) | | | T1cN2M0 | IIIA | 3 cm | | | | - |
| Pt 004 | 74 | F | Former smoker, 45 pack year | Invasive adenosquamous carcinoma (separate nodule) | | | T3N2M0 | IIIB | 2.1 cm | | | | - |
| Pt 006 | 54 | F | Nonsmoker | Pleomorphic carcinoma with adenocarcinoma | | Poor | T1cN1M0 | IIB | 2.1 cm | Exon 19 deletion | Negative | Negative | - |
| Pt 007 | 68 | M | Current 75 pack years | Adenocarcinoma | Acinar pattern | | T2aN0M0 | IB | 3 cm | Negative | Negative | Negative | - |
| Pt 008 | 79 | M | Current 100 pack years | Invasive adenocarcinoma | Papillary and hepatoid | | T2aN0M0 | IB | 3 cm | | | | + |
| Pt 009 | 82 | F | Former smoker, 50 pack years | Invasive adenocarcinoma | Lepidic, solid and glandular | Moderate | T1cN2M0 | IIIA | 3.6 cm | | | Negative | - |
| Pt 010 | 57 | F | Current, 45 pack years | Adenocarcinoma | Micropapillary, papillary and acinar | Moderate | T1bN0M0 | IA | 3.2cm | | | | + |
| Pt 012 | 82 | F | Former smoker, 60 pack years | Invasive adenocarcinoma | Acinar predominant with micropapillary pattern and colloid features | | T1aN0M0 | IA | 2.1 cm | Negative | Negative | Negative | + |
| Pt 014 | 75 | F | Nonsmoker | Invasive adenocarcinoma | Acinar predominant | | T1bN0M0 | IA | 2 cm | Exon 19 deletion | | | + |
| Pt 016 | 73 | M | Former smoker, 40 pack years | Invasive adenocarcinoma | Papillary predominant | | T2aN0M0 | IB | 1 cm | | | | + |
| Pt 017 | 74 | F | Nonsmoker | Invasive adenocarcinoma (pleural metastatic tumor) | | Well to moderate | T2bN0M1b | IV | 4.1cm | Exon 19 deletion | Negative | Negative | + |

## Supplementary Table S2. Sequence of sh*AXL* #1 and #2

| Plasmid | Sequence |
|---|---|
| sh*AXL* #1 | CCGGCTTTAGGTTCTTTGCTGCATTCTCGAGAATGCAGCAAAGAACCTAAAGTTTTT |
| sh*AXL* #2 | CCGGGCGGTCTGCATGAAGGAATTTCTCGAGAAATTCCTTCATGCAGACCGCTTTTT |

## Supplementary Table S3. Organoid medium supplements

| Additive | Vender | Cat. No. | Working concentration |
|---|---|---|---|
| EGF | PeproTech | AF-100-15 | 50 ng/ml |
| Noggin | PeproTech | 120-10C | 100 ng/ml |
| R-Spondin 1 | PeproTech | 120-44 | 500 ng/ml |
| FGF-10 | PeproTech | 100-26 | 10 ng/ml |
| FGF-basic | PeproTech | 100-18B | 10 ng/ml |
| Prostaglandin E2 | Tocris Bioscience | 2296 | 1 μM |
| Y-27632 | Sigma-Aldrich | Y0503 | 10 μM |
| Nicotinamide | Sigma-Aldrich | N0636 | 4 mM |
| A83-01 | Tocris Bioscience | 2939 | 0.5 μM |
| SB202190 | Sigma-Aldrich | S7067 | 5 μM |
| HGF | PeproTech | 100-39 | 20 ng/ml |

## Supplementary Table S4. Antibody panel of cytometry time-of-flight (CyTOF)

| Metal tag | Antigen | Clone | Vender | Cat. No. | Marker type |
|---|---|---|---|---|---|
| 89Yb | CD45 | H130 | Fluidigm | 3089003B | Immune marker |
| 141Pr | CD3 | UCHT1 | Fluidigm | 3141019B | Immune marker |
| 142Nd | CD19 | HIB19 | Fluidigm | 3142001B | Immune marker |
| 143Nd | N-Cadherin | | R&D systems | AF6426 | EMT |
| 144Nd | ALDH1A1 | 703410 | R&D Systems | MAB5869 | Stemness |
| 145Nd | CD163 | GHI/61 | Fluidigm | 3145010B | Immune marker |
| 146Nd | ZO-2 | 3E8D9 | ThermoFisher Scientific | 374700 | EMT |
| 148Nd | CD16 | 3G8 | Fluidigm | 3148004B | Immune marker |
| 149Sm | CD200 | OX104 | Fluidigm | 3149007B | Stromal marker |
| 150Ne | CD86 | IT2.2 | Fluidigm | 3150020B | Immune marker |
| 151Eu | CD133 | 170411 | R&D Systems | MAB11331-100 | Stemness |
| 152Sm | SMAD2 | 31H15L4 | ThermoFisher Scientific | 700048 | Signaling |
| 153Eu | JAK1 | 413104 | R&D Systems | MAB4260 | Signaling |
| 155Gd | Fibronectin | 2F4 | ThermoFisher Scientific | MA517075 | EMT |
| 156Gd | Vimentin | | R&D systems | MAB2105 | EMT |
| 158Gd | pSTAT3 | 4/p-stat3 | Fluidigm | 3158005A | Signaling |
| 159Tb | CD90 | 5E10 | Fluidigm | 3159007B | Stromal marker |
| 160Gd | OCT3/4 | 240408 | R&D Systems | MAB1759 | Stemness |
| 161Dy | AXL | | R&D systems | AF154 | Signaling |
| 162Dy | CD66b | 80H3 | Fluidigm | 3162023B | Immune marker |
| 163Dy | CD105 | 43A3 | Fluidigm | 3163005B | Endothelial marker |
| 164Dy | SMAD4 | 253343 | R&D Systems | MAB2097 | Signaling |
| 165Ho | TGFBR2 | | R&D Systems | AF-241 | Signaling |
| 166Er | SNAI1 | | Sigma | SAB 2108482 | EMT |
| 167Er | TWIST1 | 927403 | R&D systems | MAB6230 | EMT |
| 168Er | β-catenin | 196624 | R&D systems | MAB13292 | Signaling |
| 169Tm | Nanog | N31355 | Fluidigm | 3169014A | Stemness |
| 170Er | STRO-1 | STRO-1 | R&D Systems | MAB1038 | Stromal marker |
| 171Yb | CD44 | IM7 | Fluidigm | 3171003B | Stemness |
| 172Yb | PECAM | HEC7 | ThermoFisher Scientific | MA3100 | EMT, endothelial marker |
| 173Yb | EPCAM | | R&D systems | AF960 | EMT, epithelial marker |
| 174Yb | Keratin 8/18 | C51 | Fluidigm | 3174014A | EMT, epithelial marker |
| 175Lu | CD14 | M5E2 | Fluidigm | 3175015B | Immune marker |
| 176Yb | CD56 | CMSSB | Fluidigm | 3176003B | Immune marker |

## Supplementary References


1. Smith J RM, Acosta K, Vennapusa B, Mistry A, Martin G, Yates A, Hnatyszyn HJ. Quantitative and qualitative characterization of Two PD-L1 clones: SP263 and E1L3N. Diagn Pathol **2016**;11
2. Allred DC, Harvey JM, Berardo M, Clark GM. Prognostic and predictive factors in breast cancer by immunohistochemical analysis. Modern pathology : an official journal of the United States and Canadian Academy of Pathology, Inc **1998**;11:155-68
3. Gao J, Aksoy BA, Dogrusoz U, Dresdner G, Gross B, Sumer SO*, et al.* Integrative analysis of complex cancer genomics and clinical profiles using the cBioPortal. Sci Signal **2013**;6:pl1
4. Cerami E, Gao J, Dogrusoz U, Gross BE, Sumer SO, Aksoy BA*, et al.* The cBio cancer genomics portal: an open platform for exploring multidimensional cancer genomics data. Cancer discovery **2012**;2:401-4
5. Dobin A, Davis CA, Schlesinger F, Drenkow J, Zaleski C, Jha S*, et al.* STAR: ultrafast universal RNA-seq aligner. Bioinformatics (Oxford, England) **2013**;29:15-21
6. Li B, Dewey CN. RSEM: accurate transcript quantification from RNA-Seq data with or without a reference genome. BMC bioinformatics **2011**;12:323
7. Fabregat A, Sidiropoulos K, Viteri G, Forner O, Marin-Garcia P, Arnau V*, et al.* Reactome pathway analysis: a high-performance in-memory approach. BMC bioinformatics **2017**;18:142
8. Mi H, Poudel S, Muruganujan A, Casagrande JT, Thomas PD. PANTHER version 10: expanded protein families and functions, and analysis tools. Nucleic acids research **2016**;44:D336-42
9. Zhao M, Kong L, Liu Y, Qu H. dbEMT: an epithelial-mesenchymal transition associated gene resource. Sci Rep **2015**;5:11459
10. Shen Y, Yao H, Li A, Wang M. CSCdb: a cancer stem cells portal for markers, related genes and functional information. Database (Oxford) **2016**;2016
11. Martowicz A, Spizzo G, Gastl G, Untergasser G. Phenotype-dependent effects of EpCAM expression on growth and invasion of human breast cancer cell lines. BMC Cancer **2012**;12:501

# Supplementary Fig. S1

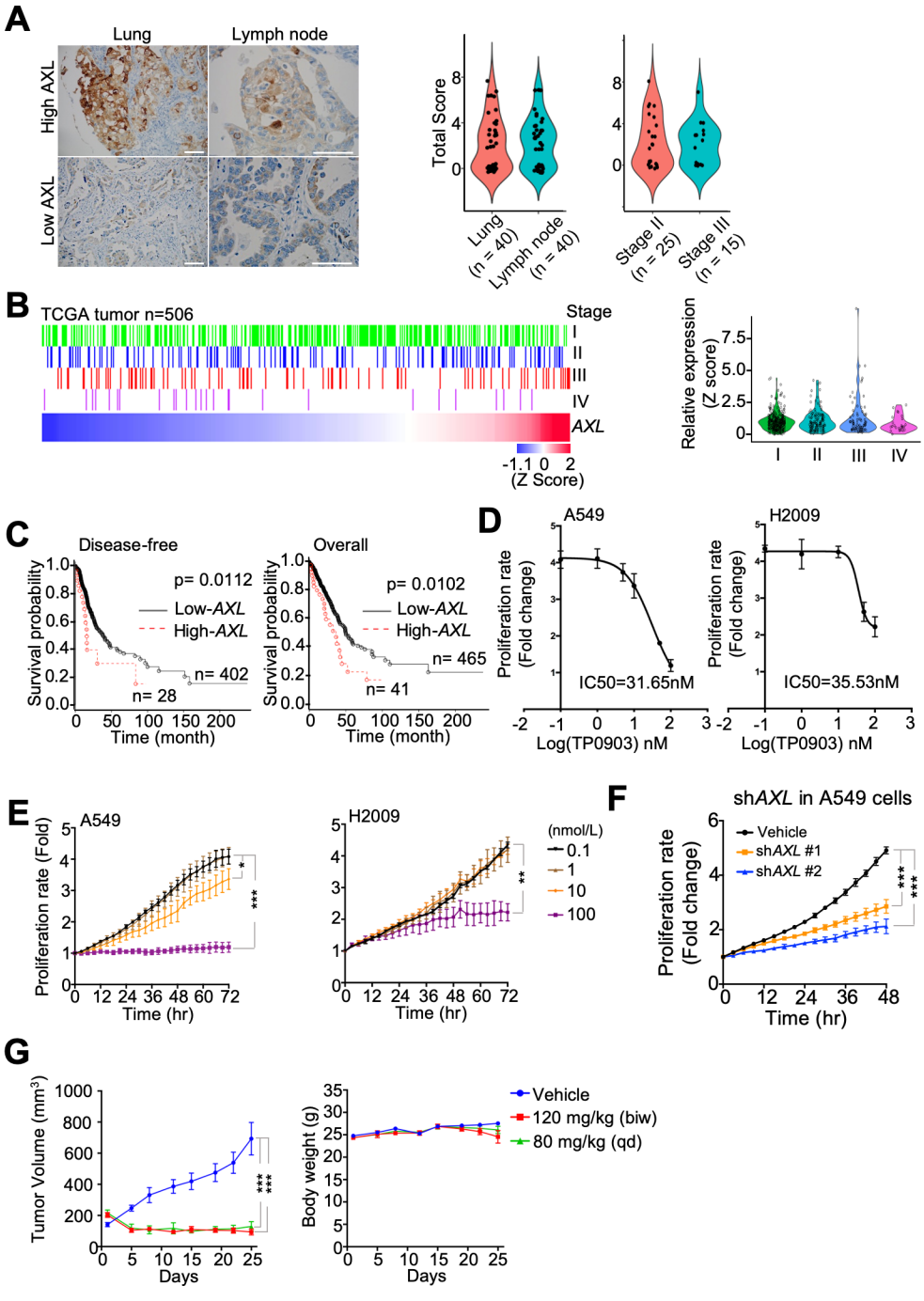

# Supplementary Fig. S2

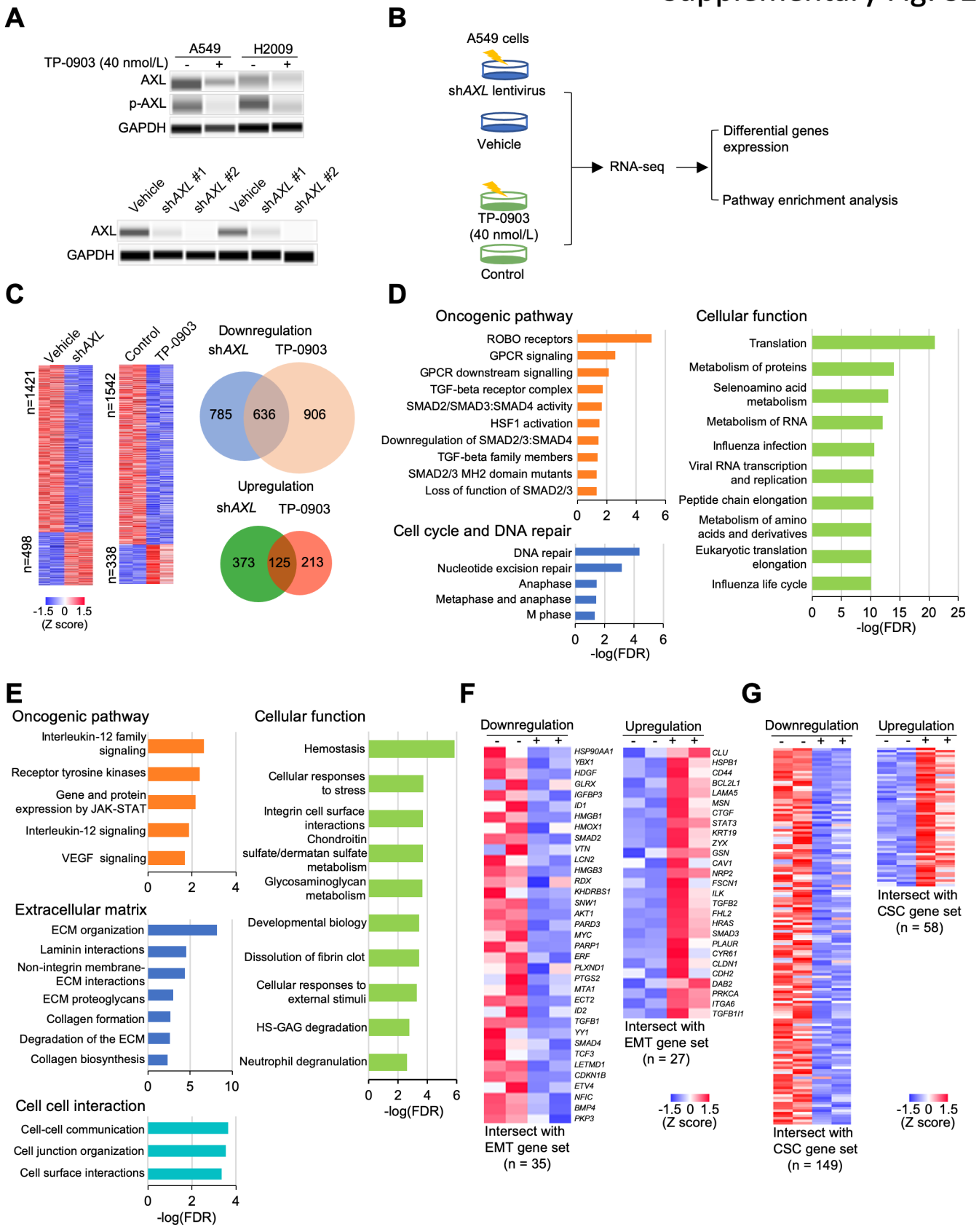

# Supplementary Fig. S3

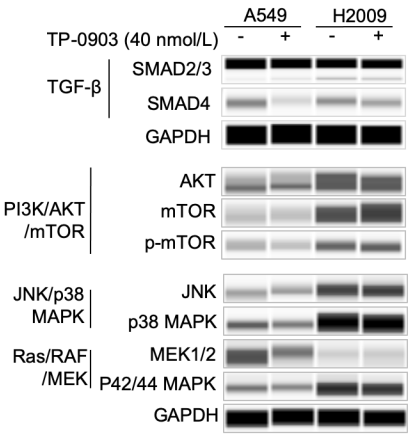

# Supplementary Fig. S4

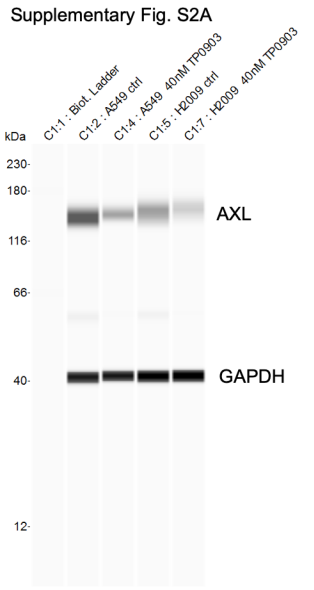


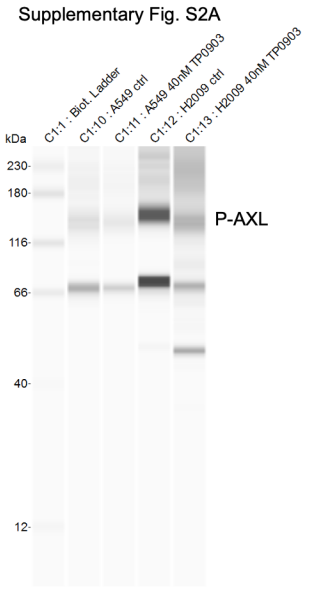


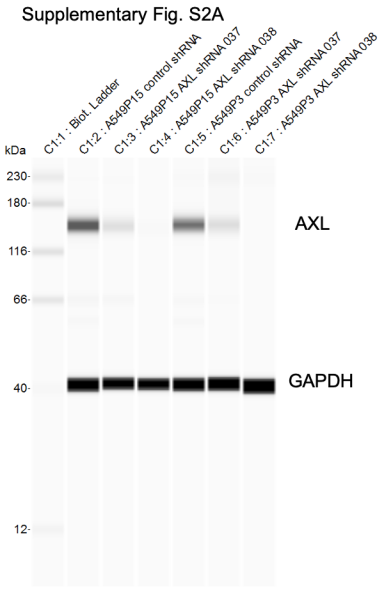


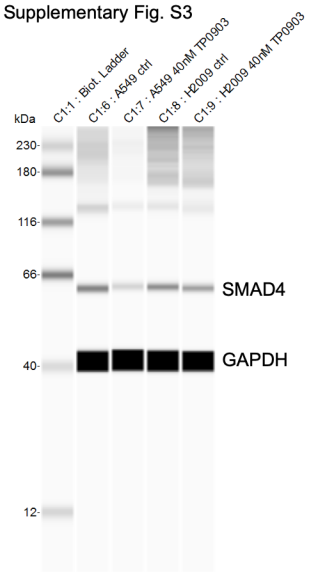


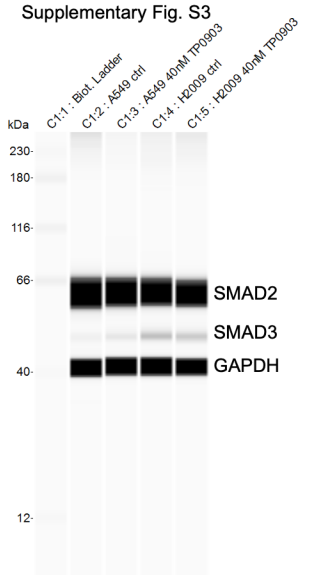


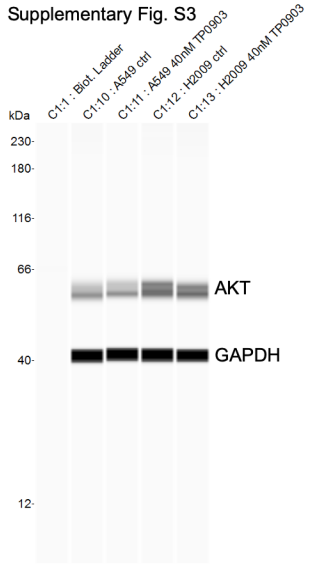


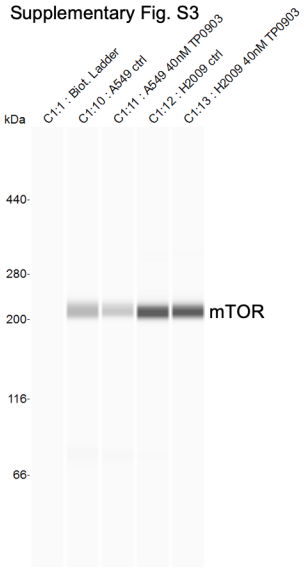


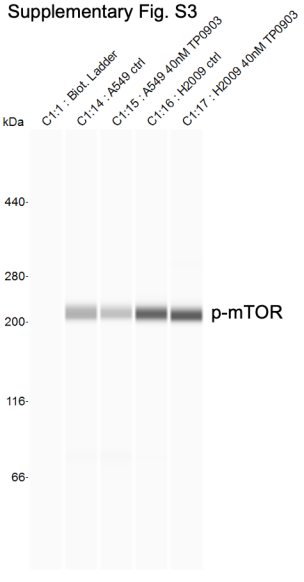


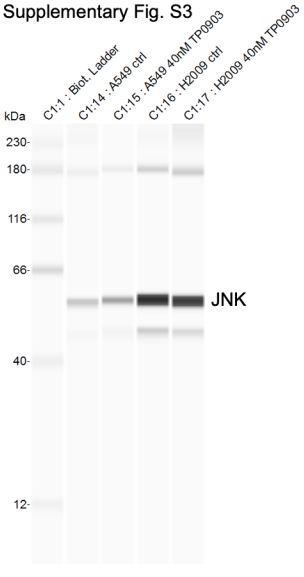

# Supplementary Fig. S4 - continue

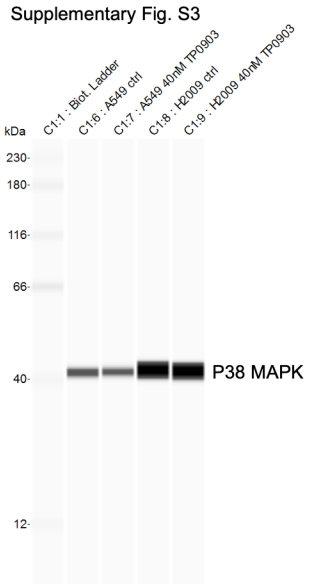


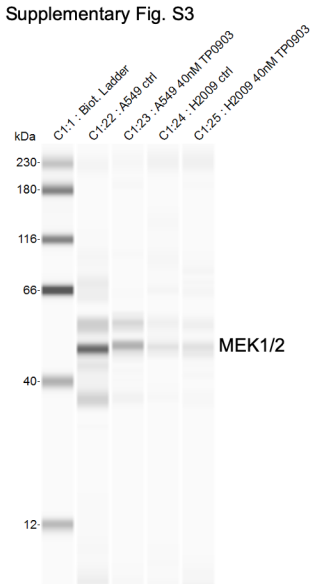


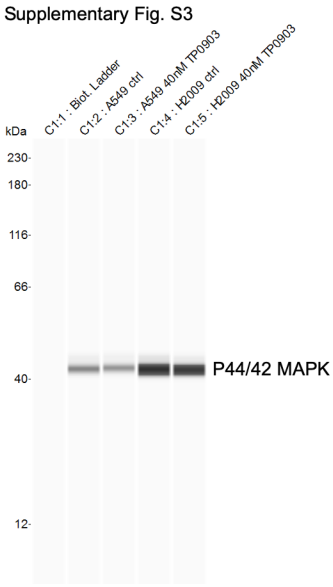

# Supplementary Fig. S5

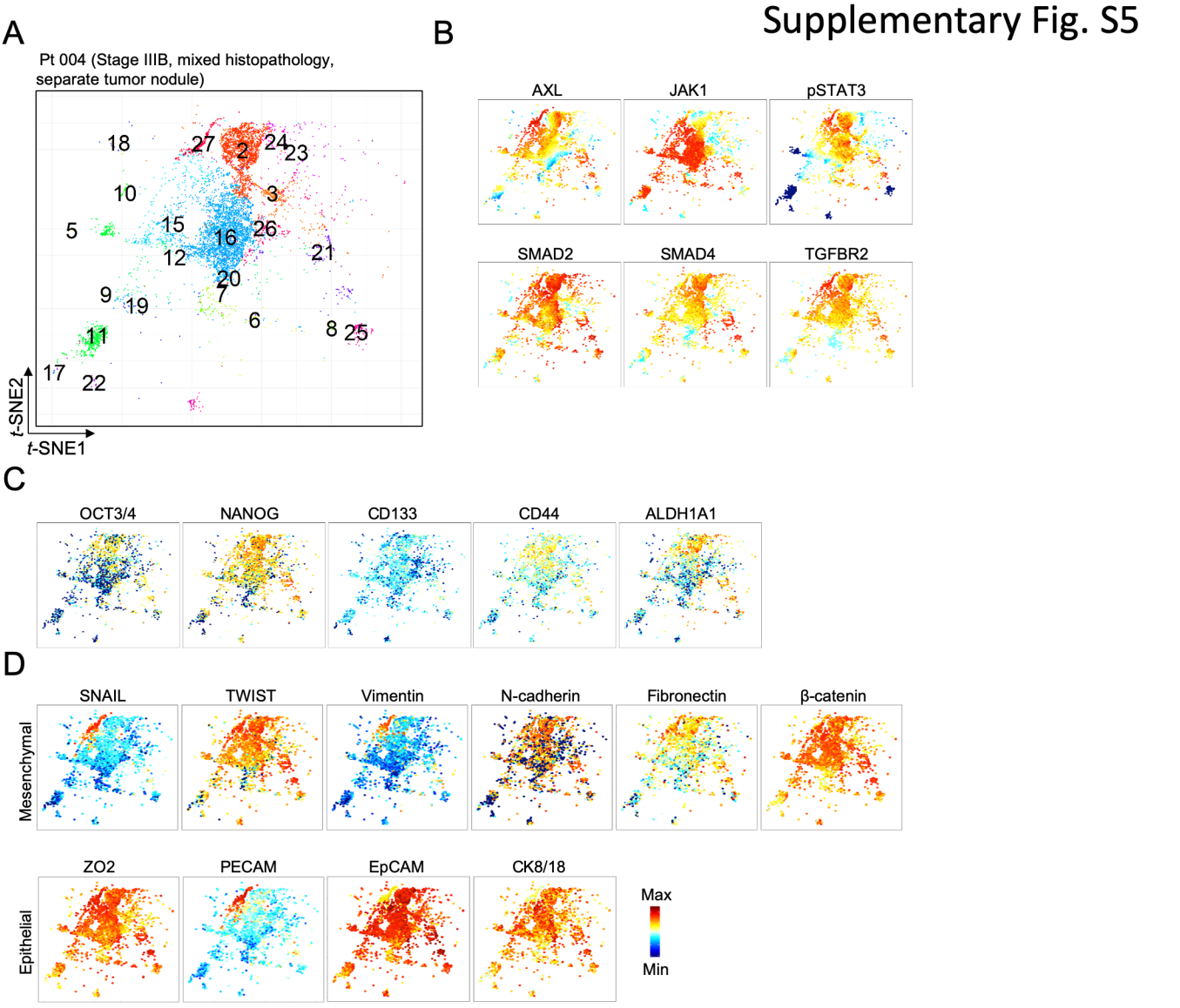

# Supplementary Fig. S6

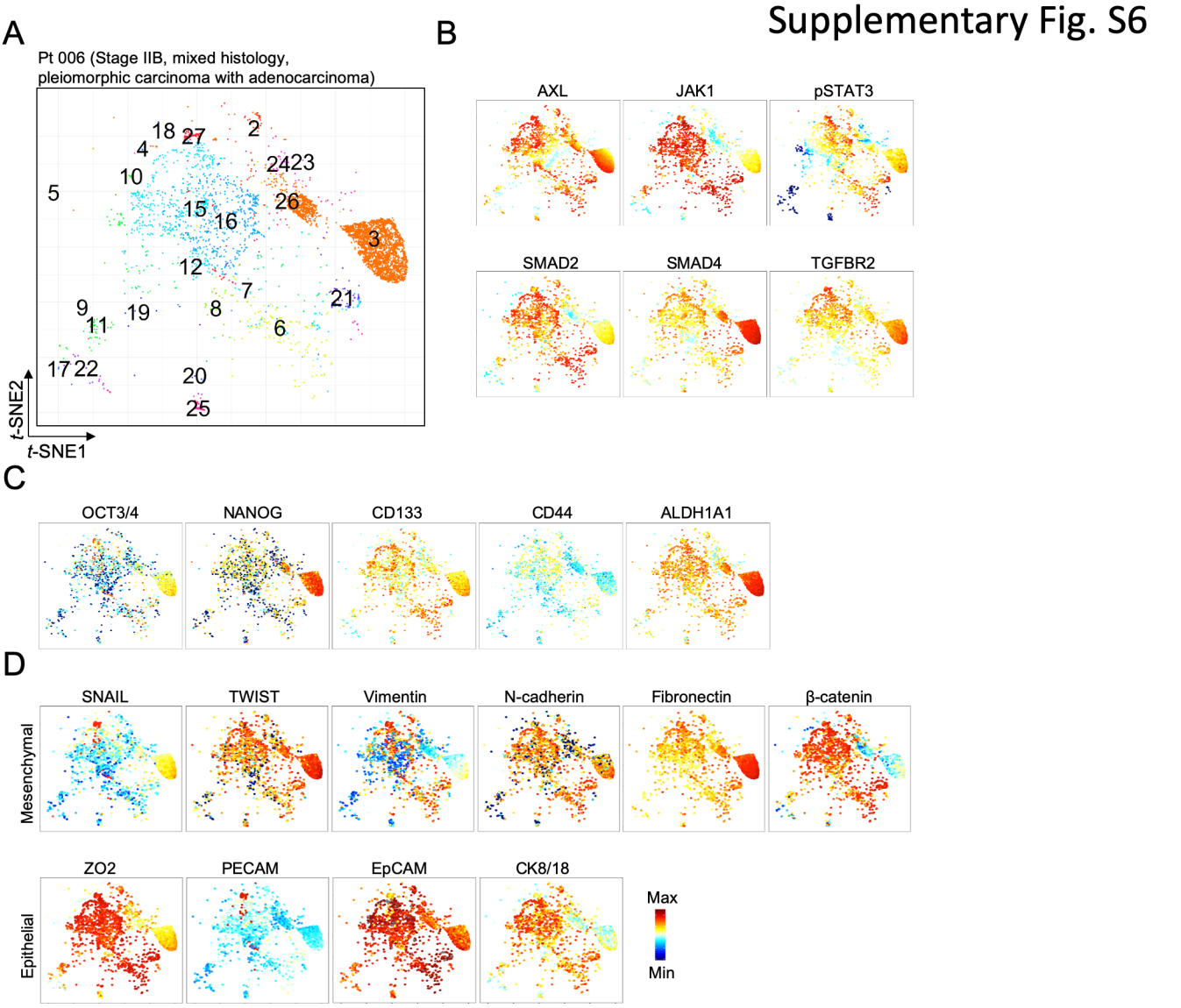

# Supplementary Fig. S7

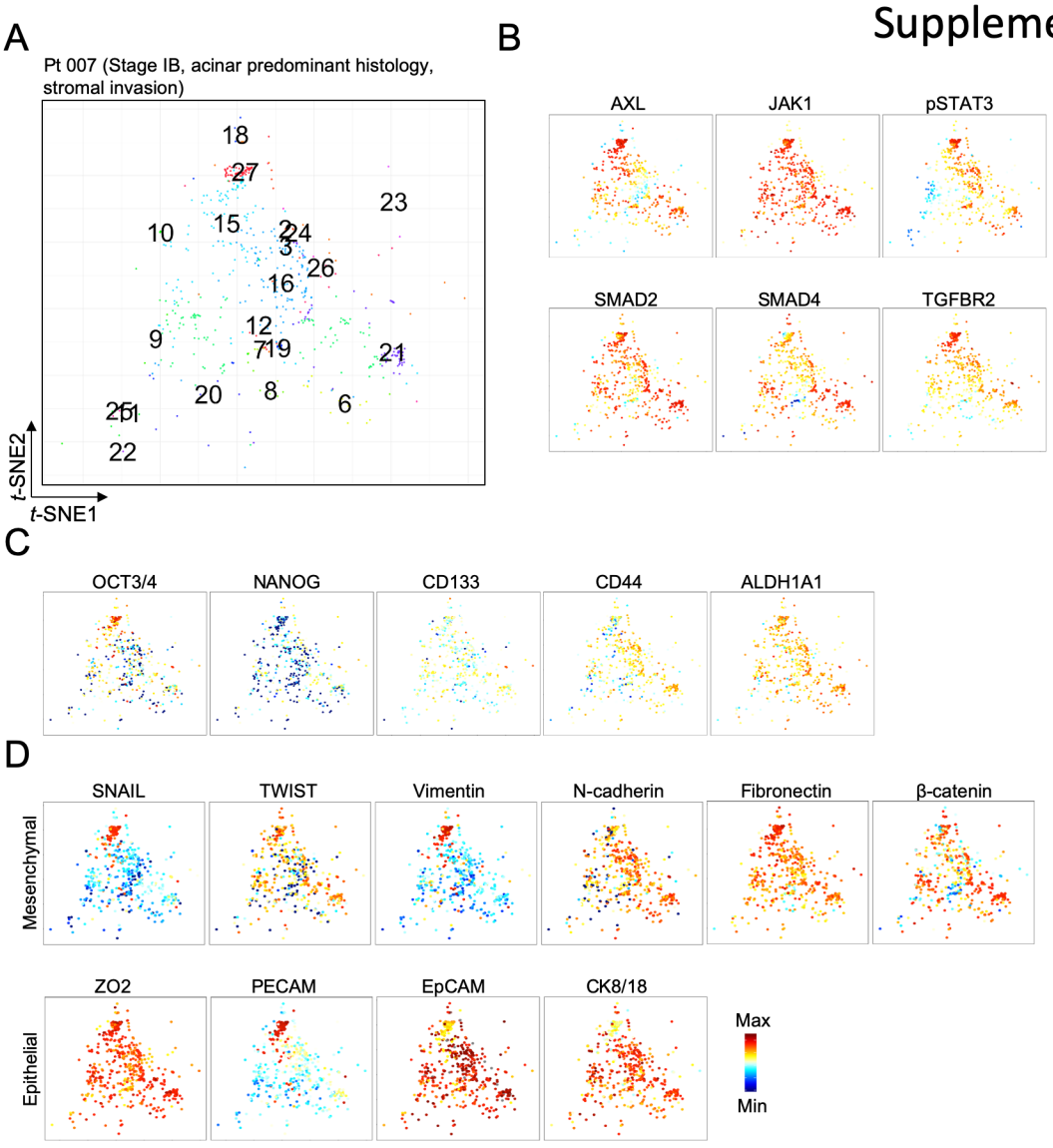

# Supplementary Fig. S8

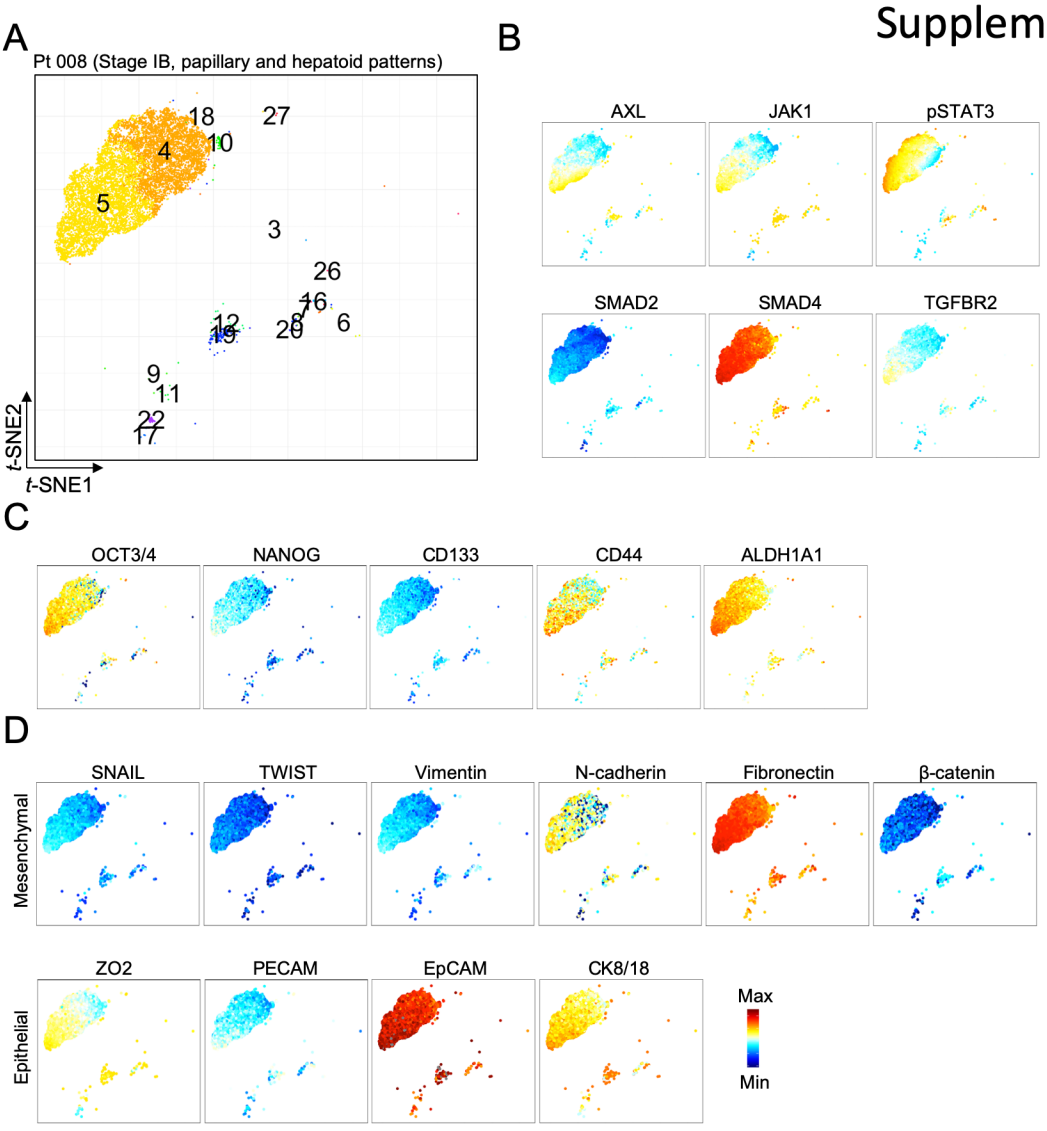

# Supplementary Fig. S9

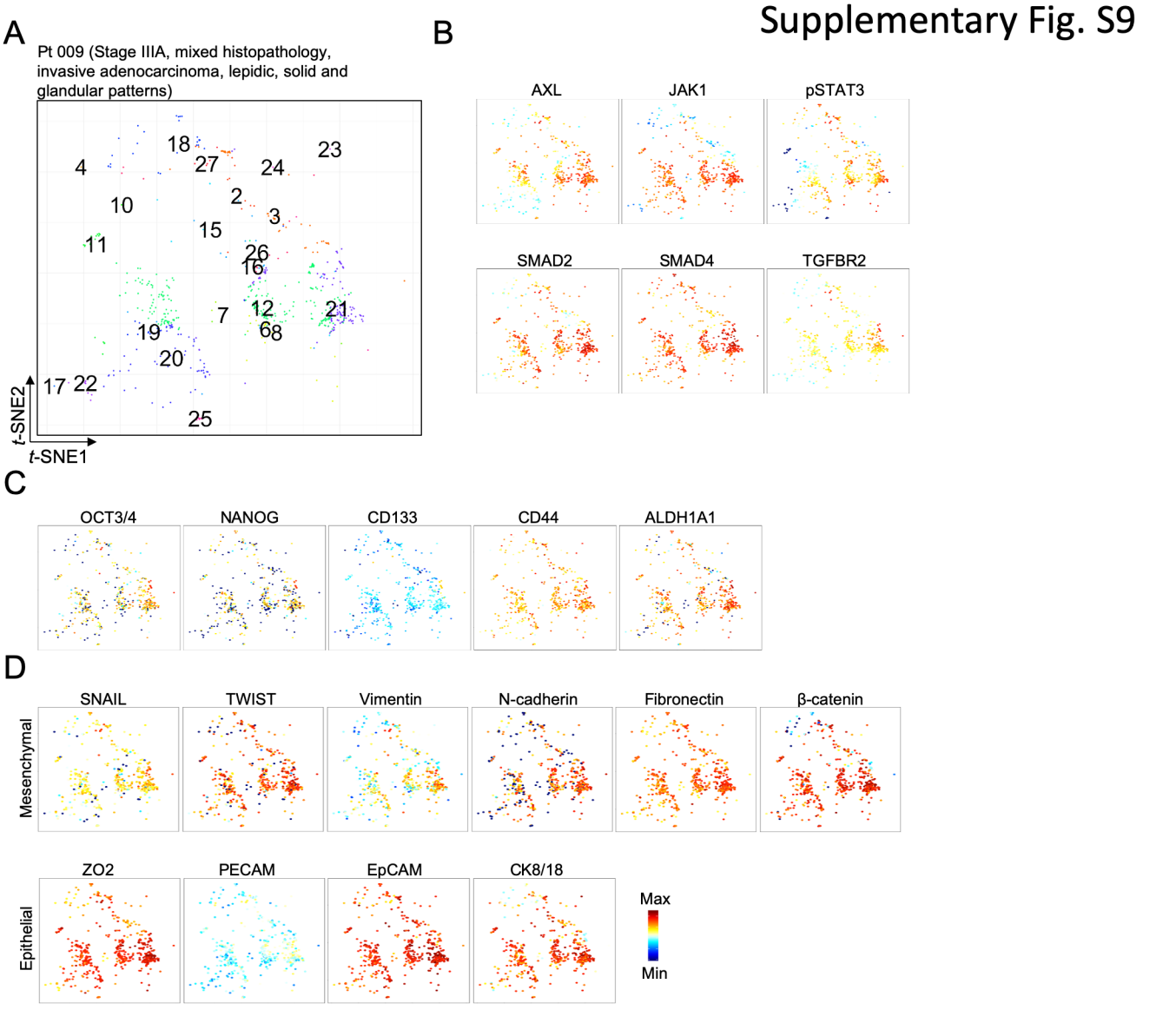

# Supplementary Fig. S10

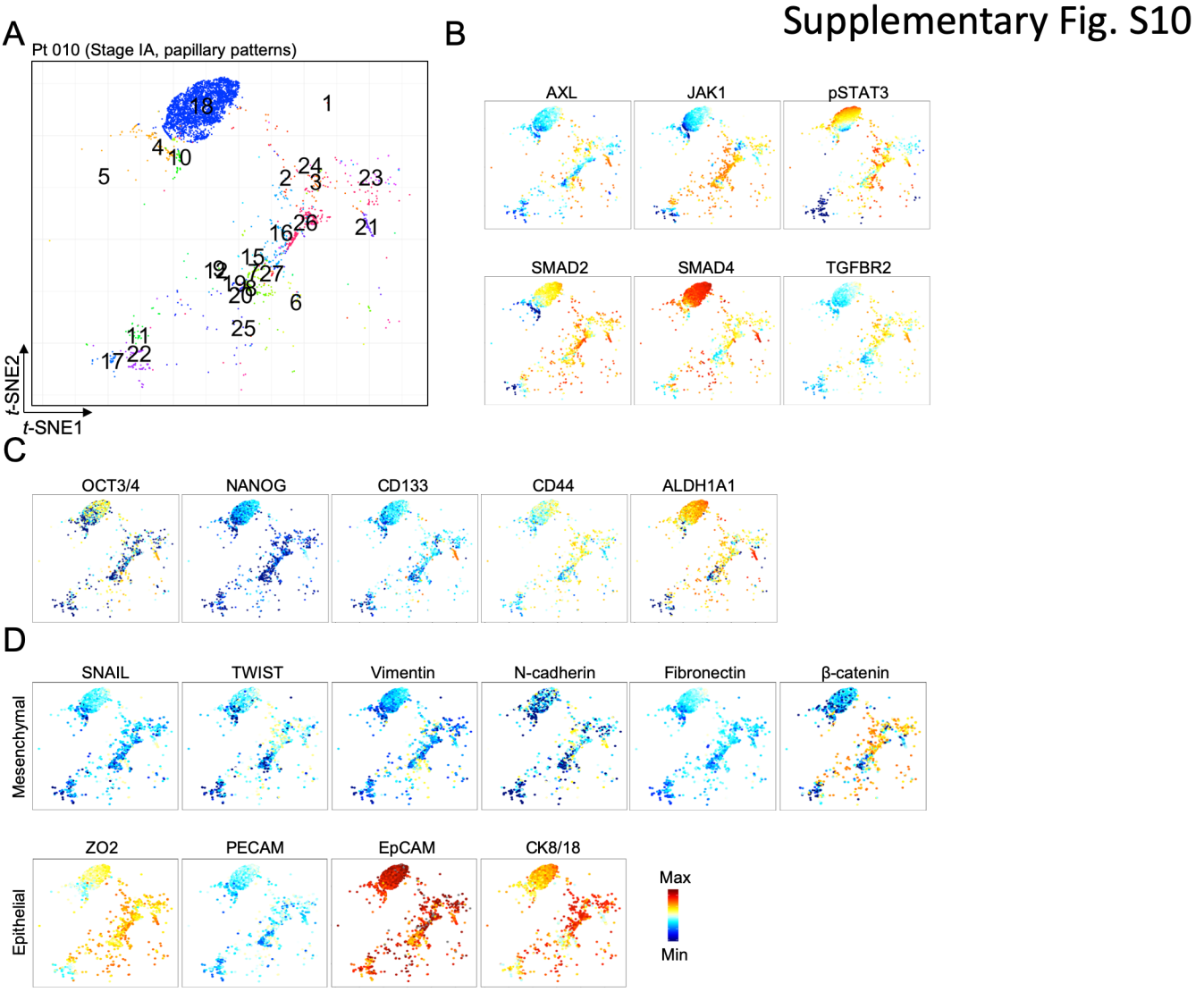

# Supplementary Fig. S11

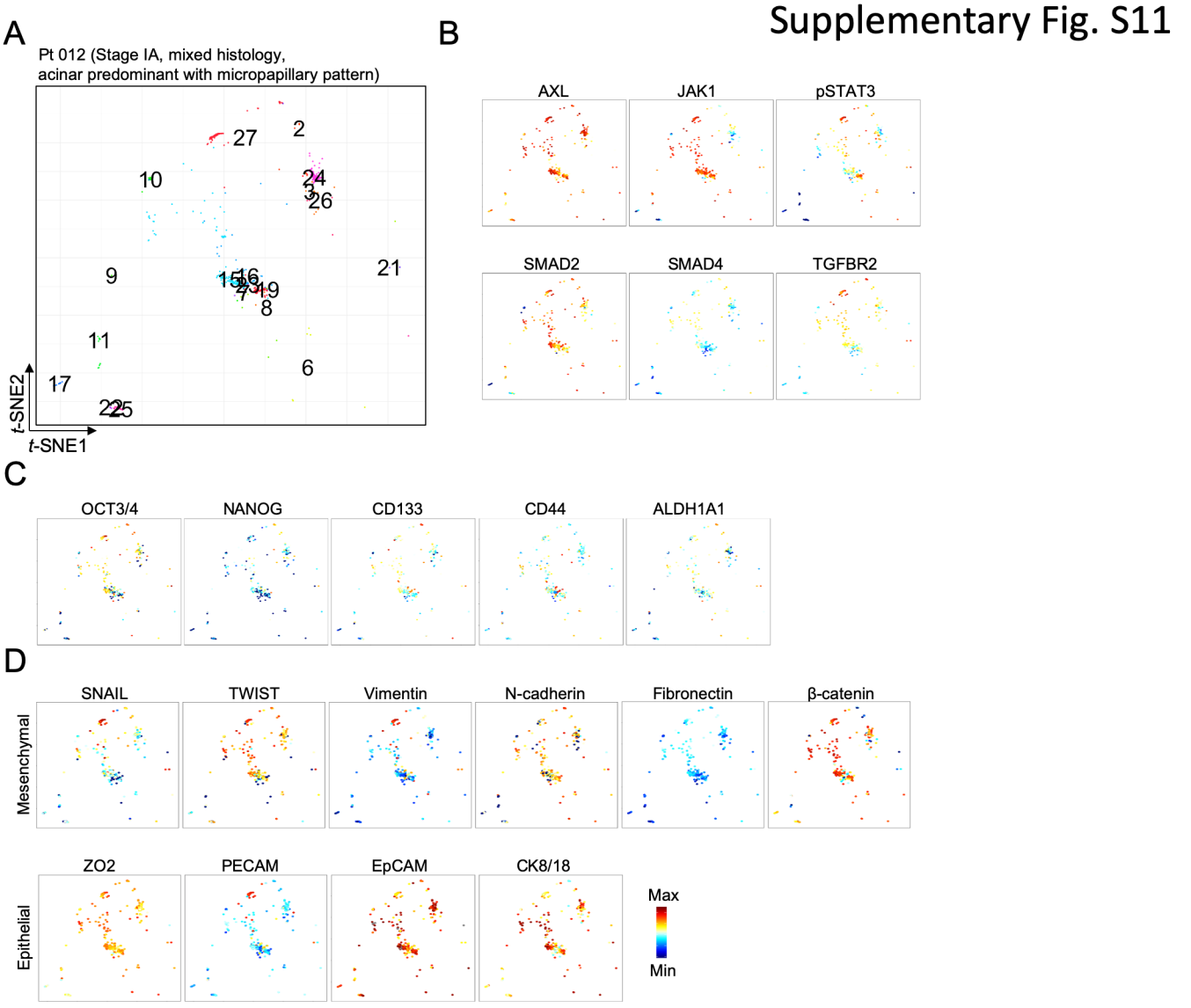

# Supplementary Fig. S12

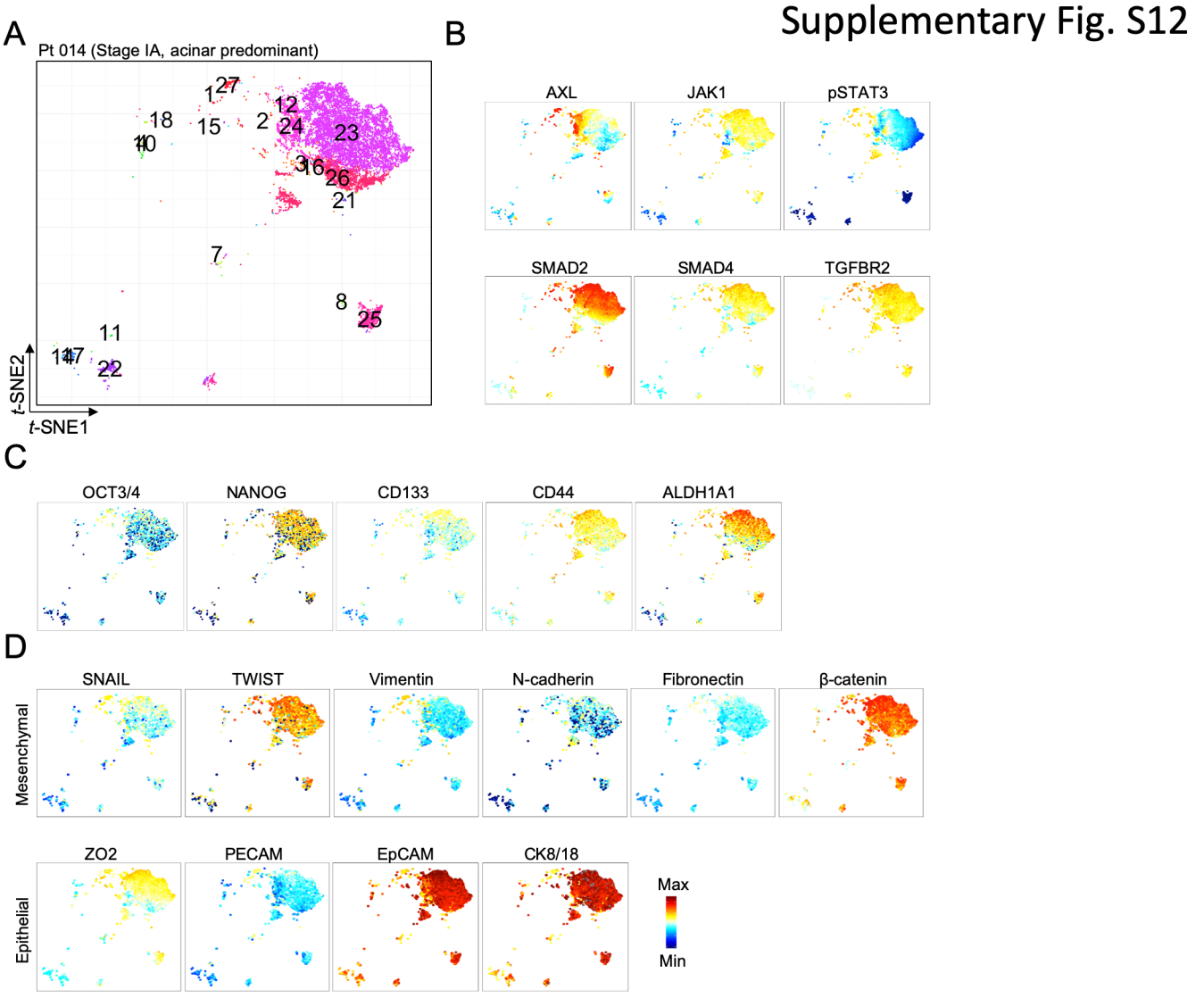

# Supplementary Fig. S13

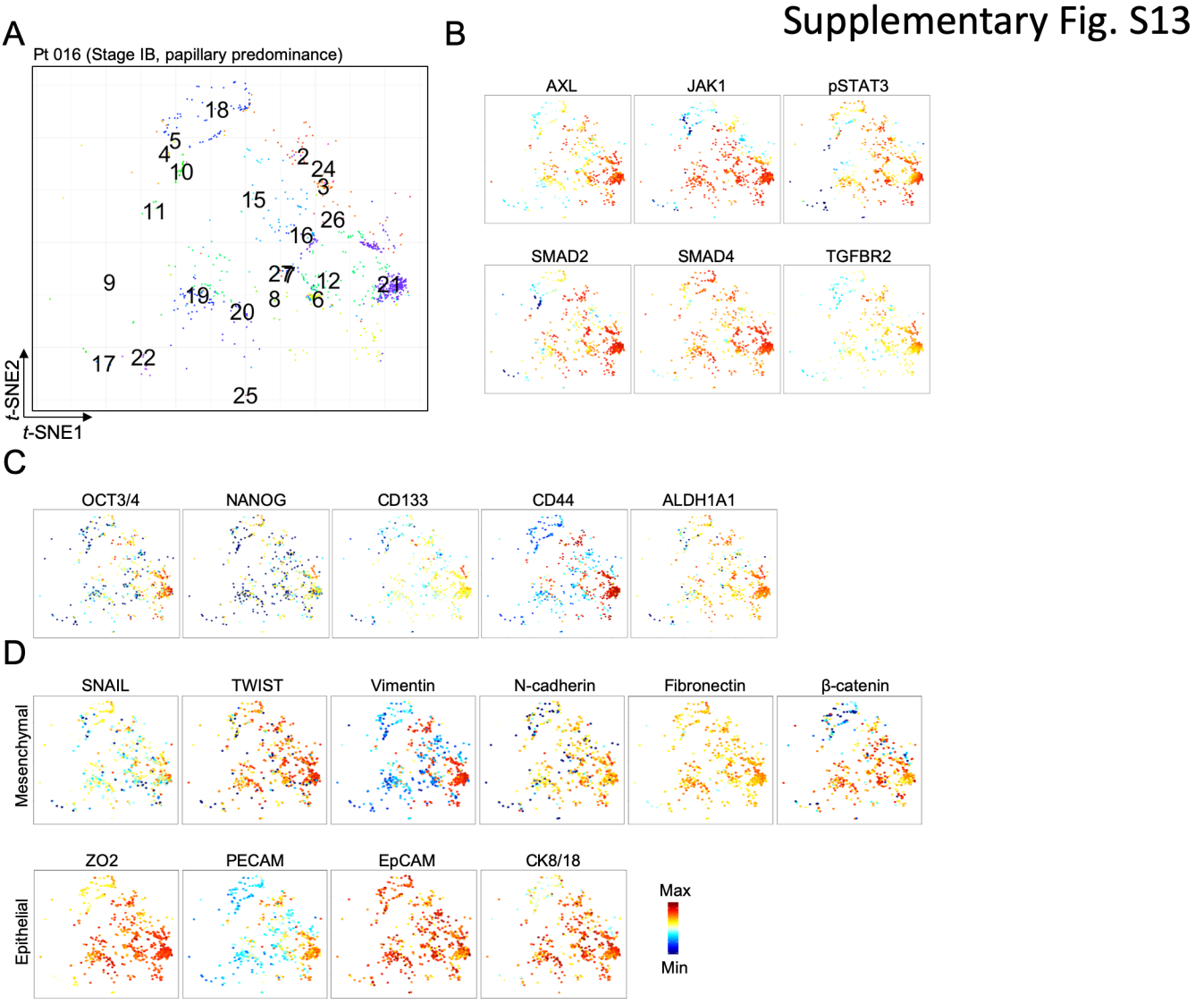

# Supplementary Fig. S14

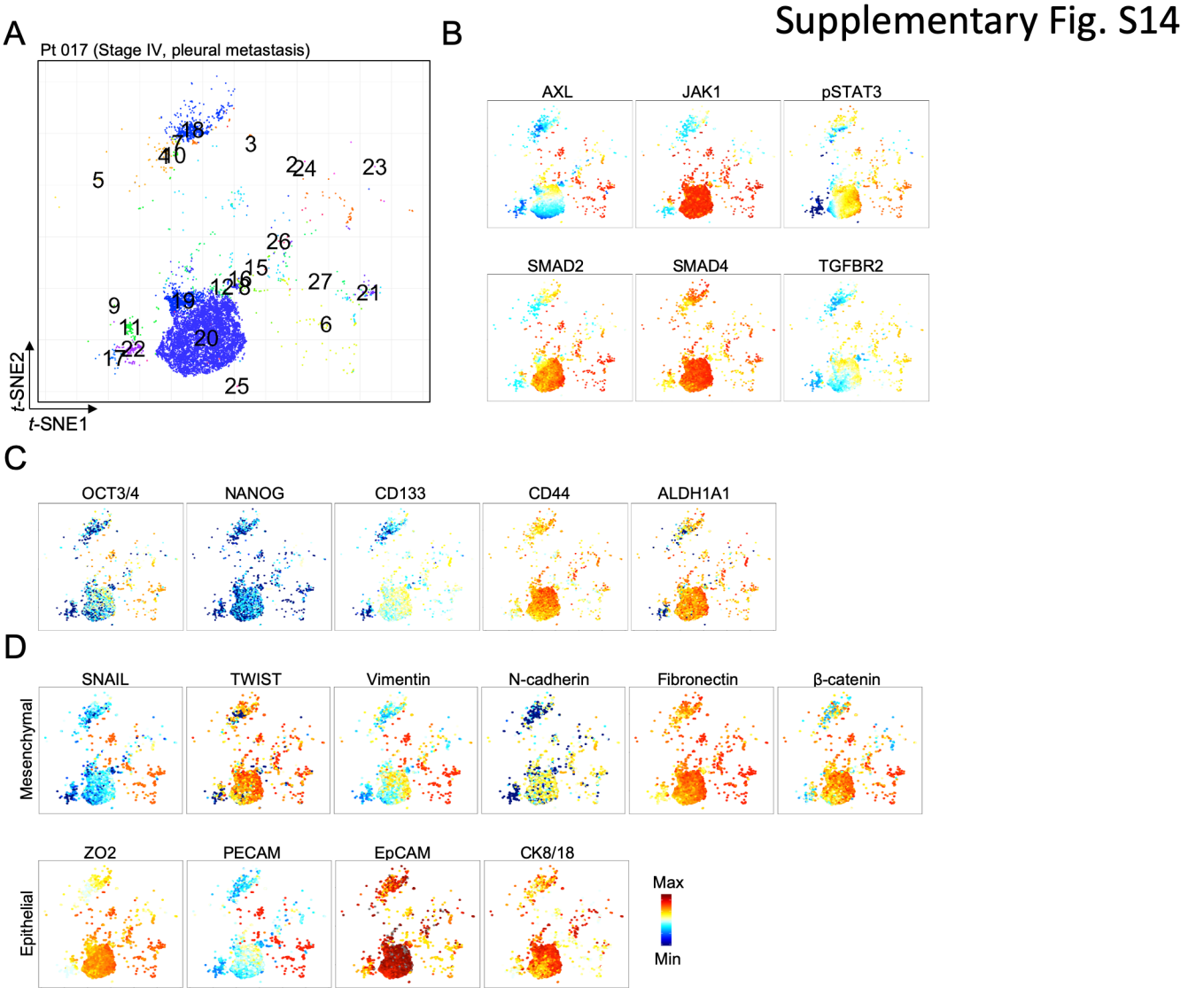

# Supplementary Fig. S15

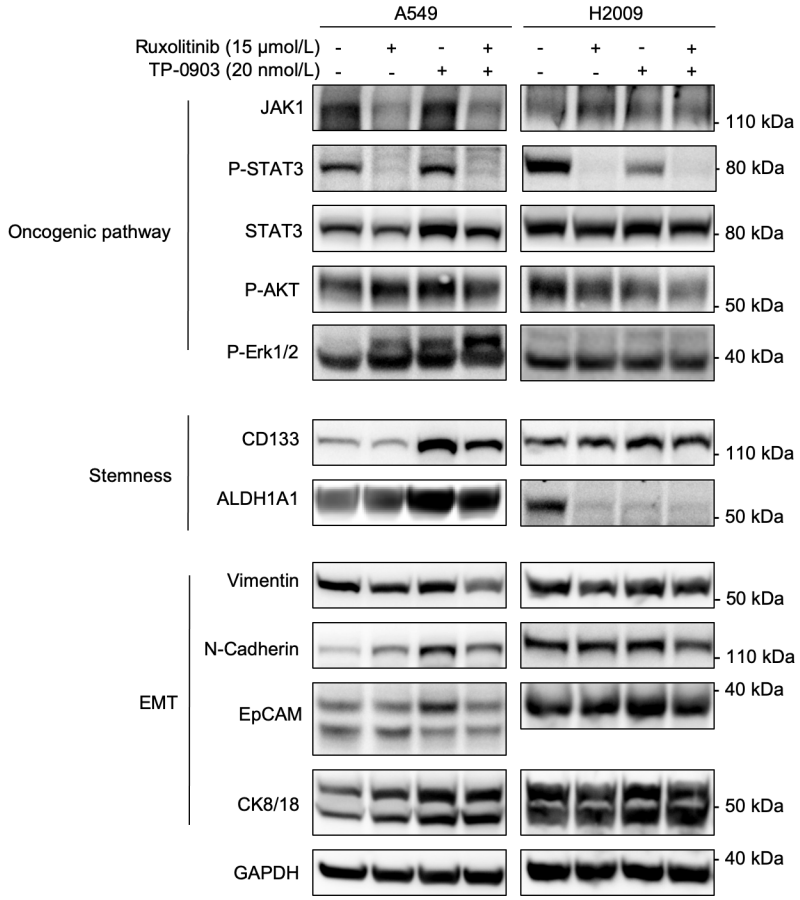

# Supplementary Fig. S16